

# Novel Compact and High Selectivity Dual-band BPF with Wide Stopband

Lei WANG<sup>1</sup>, Bo-Ran GUAN<sup>2</sup>

<sup>1</sup> School of Electronic Engineering, Xidian University, Xi'an, Shaanxi, 710071, China

<sup>2</sup> Institute of Antenna and Microwave, Hangzhou Dianzi University, Hangzhou, Zhejiang, 310018, China

wanglei.em@gmail.com, brguan@hdu.edu.cn

**Abstract.** *A novel type of compact and high selectivity dual-band bandpass filter (BPF) incorporating a dual-mode defected ground structure resonator (DDGSR) and a dual-mode open-stub loaded stepped impedance resonator (DOLSIR) is proposed in this paper. Utilizing capacitive source-load coupling and the intrinsic characteristics of the two types of dual-mode resonators, compact dual-band BPF with multi transmission zeros near the passband edges as well as a wide stopband which can be used to achieve high selectivity is realized. An experimental dual-band BPF located at 2.4 and 3.2 GHz was designed and fabricated. The validity of the design approach is verified by good agreement between simulated and measurement results.*

## Keywords

Dual-mode, dual-band, bandpass, defected ground structure.

## 1. Introduction

Dual-band BPFs attracted much attention recently because they are the key components in modern multimode wireless communication systems. Many methods for designing dual-band BPFs have been investigated and reported. Combination of a bandpass filter and a bandstop filter in series [1] or two bandpass filters which have individual passband in parallel [2], can construct a dual-band filter. But this type of filters has drawbacks in relatively large filter size. The defected stepped impedance resonators [3] or meander open-loop resonators [4] are introduced in the dual-band filter design to reduce the filter size; while they have a relatively large number of resonators. Dual-band filters using the stepped impedance resonators [5-6], dual-mode resonators [7-9] or embedded resonators [10-11], which coupled with each other have less resonators and compact size. However, the design procedure is complicated because the coupling co-efficiencies of the resonators at two separate passbands are difficult to be fulfilled simultaneously. Another widely researched method to design dual-band filter is using two dual-mode resonators,

which are not coupled with each other [12-14]. This type of dual-band BPFs has advantages in design flexibility that two passbands can be designed separately and changed individually. Moreover, in [15], dual-band BPF using two E-shaped dual-mode resonators with T-shaped feed lines can achieve two passbands and a wide upper stopband simultaneously, however, as there is only one transmission zero near the passband edges, the selectivity needs to be improved.

In this paper, a novel design method of compact and high selectivity dual-band BPFs using the DDGSR and DOLSIR is presented. High selectivity is achieved by multi transmission zeros near the passband edges, which are created by capacitive source-load coupling and the intrinsic characteristics of the resonators. Meanwhile, using the wideband spurious frequency suppression characteristics of the resonators, wide upper stopbands are realized simultaneously to improve the selectivity. Furthermore, the second passband frequency can be shifted conveniently in a wide range by changing the parameters of the DOLSIR while not significantly affecting the first passband and out-of-band performances. Finally, an experimental dual-band BPFs have been simulated and fabricated. The measured results agree well with the simulated ones.

## 2. Filter Design

### 2.1 Resonator Analysis

Dual-mode resonators, such as the DDGSR and DOLSIR which have two non-degenerate modes, have advantages in circuit size and design flexibility. The schematics of the two types of dual-mode resonators are shown in Fig. 1. The top and bottom metal regions are depicted in black and gray, respectively.

According to [16], the first two resonant frequencies of the DDGSR are the resonant frequencies of the slot line resonator (SLR) and the coplanar stepped impedance resonator (CSIR) inside the slot line, respectively. The equivalent circuit models for two different resonant modes of the DDGSR are shown in Fig. 2(a). Therefore, the resonant conditions of the first two resonant frequencies of the DDGSR will be

$$\theta_1 = \pi \quad (\text{at } f = f_{1SLR}), \quad (1)$$

$$\tan \theta_2 \tan \theta_3 = Z_2/Z_3 \quad (\text{at } f = f_{1CSIR}) \quad (2)$$

where  $Z_1, Z_2, Z_3$  and  $\theta_1, \theta_2, \theta_3$  represent the characteristic impedances and the electric lengths as shown in Fig. 1(a). From (1) and (2), the two resonant frequencies of the DDGSR are independent and can be changed separately.

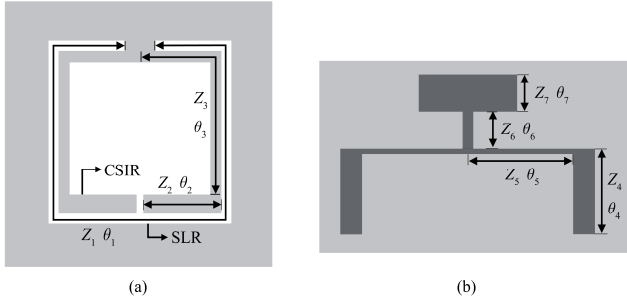


**Fig. 1.** Schematics of two types of dual-mode resonators: (a) DDGSR, (b) DOLSIR.

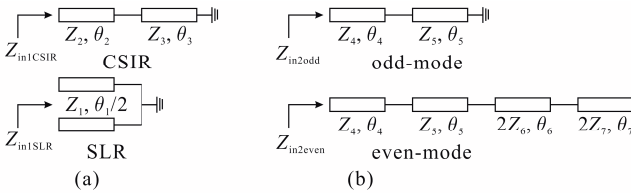


**Fig. 2.** Equivalent circuit models for different modes of the two types of dual-mode resonators. (a) DDGSR, (b) DOLSIR.

The odd- and even-mode method is applied to analyze the DOLSIR, which has the equivalent circuit model as shown in Fig. 2(b). The resonant condition of the first two resonant frequencies will be

$$\tan \theta_4 \tan \theta_5 = Z_4/Z_5 \quad (\text{at } f = f_{2odd}), \quad (3)$$

$$\frac{Z_5}{2Z_6} \cdot \frac{Z_4 - Z_5 \tan \theta_4 \tan \theta_5}{Z_4 \tan \theta_5 + Z_5 \tan \theta_4} = \frac{Z_6 \tan \theta_6 \tan \theta_7 - Z_7}{Z_6 \tan \theta_7 + Z_7 \tan \theta_6} \quad (\text{at } f = f_{2even}) \quad (4)$$

where  $Z_4, Z_5, Z_6, Z_7$  and  $\theta_4, \theta_5, \theta_6, \theta_7$  represent the characteristic impedances and electric lengths shown in Fig. 1(b).

## 2.2 Filter Construction

Simple microstrip open-stubs with adjacent open ends are chosen to be used as common input/output feed structures to excite the two types of dual-mode resonators mentioned above and introduce capacitive source load coupling simultaneously, as shown in Fig. 3. The coupling schemes for the two passbands are depicted in Fig. 4. The two passbands can be designed separately and the frequency responses of different types of BPFs are shown in Fig. 5(a).

The DDGSR is chosen to design the first passband since it has an advantage in generating a very wide upper stopband [16]. The coupling scheme for the first passband is depicted in Fig. 4(a). The phase shift of the SLR is  $+90^\circ$

in the lower stopband since the behavior of the parallel LC resonator formed by the SLR is inductive at low frequencies. Therefore, incorporating  $-90^\circ$  phase shift introduced by the capacitive source load coupling, a transmission zero ( $Tz_1$ ) will be generated in the lower stopband. With its inherent transmission zero ( $Tz_2$ ) chosen to be in the upper stopband by  $f_{1SLR} < f_{1CSIR}$ , two transmission zeros on both sides of the first passband can be realized to achieve high selectivity, as shown in Fig. 5(a).

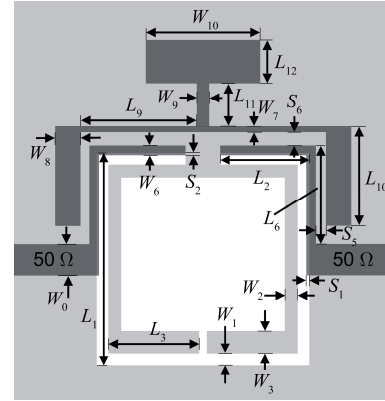


**Fig. 3.** Layout of the proposed dual-band BPF.

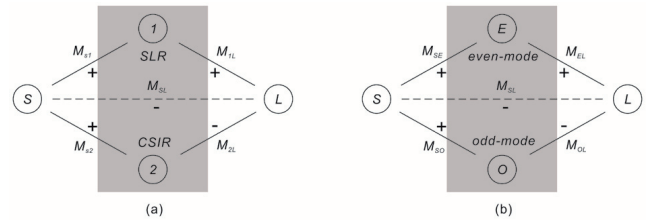


**Fig. 4.** Coupling schemes for (a) first passband and (b) second passband.

The second passband is designed using the DOLSIR. With the same feed structures as for the first passband, a single-band BPF with capacitive source load coupling scheme can be achieved. The coupling scheme for the second passband is depicted in Fig. 4(b). For the DOLSIR which has an inherent zero ( $Tz_3$ ) [17], the capacitive source load coupling can engender an additional transmission zero ( $Tz_4$ ) in the upper stopband [18], and a high selectivity BPF can be realized. As shown in Fig. 5(a), two passbands of the dual-band BPF can be designed separately. By combining the two single-band BPFs with the common input/output feed lines, a dual-mode dual-band BPF can be realized.

Moreover, as depicted in Fig. 5(b), the second passband frequency can be shifted conveniently by changing the parameters  $L_{10}$  and  $L_{12}$  which corresponds to the electric length  $\theta_4$  and  $\theta_7$ . By changing  $L_{10}$  from 3.5 to 0.2 mm, the odd-mode resonant frequency of the DOLSIR can be shifted from 3.2 to 5.2 GHz continuously. And the second passband can be generated with adjustment of the parameter  $L_{12}$ , while the first passband has been hardly affected. An intrinsic characteristic of the DOLSIR is that, it has an inherent zero which is associated with the even-mode

resonant frequency of the resonator which is controlled by  $L_{12}$ . So it is convenient to allocate the inherent transmission zero in the higher side of the second passband ( $f_{2odd} < f_{2even}$ ) to improve the upper stopband performance or in the lower side of the second passband ( $f_{2odd} > f_{2even}$ ) to improve the isolation between the two passbands.

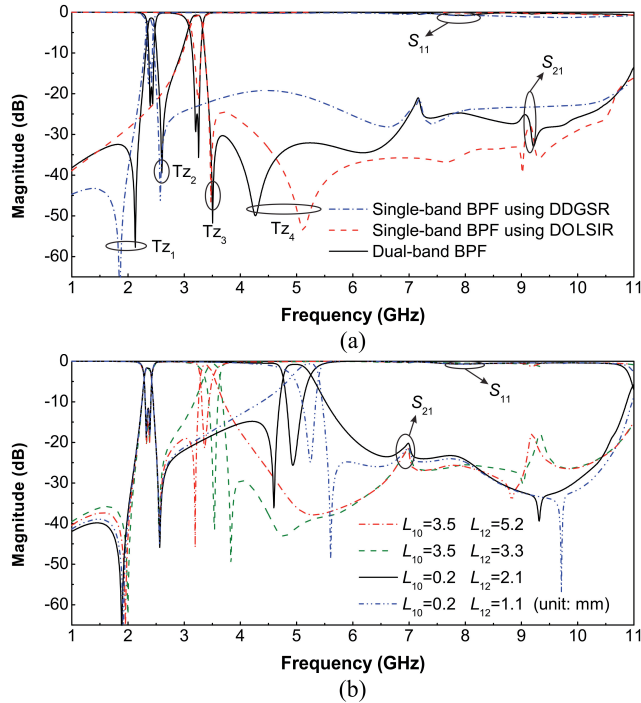


**Fig. 5.** Simulated frequency responses of the single- and dual-band BPFs using the DDGSR and DOLSIR: (a) Single- and dual-band BPFs, (b) Dual-band BPF against  $L_{10}$ ,  $L_{12}$ .

### 3. Experimental Results

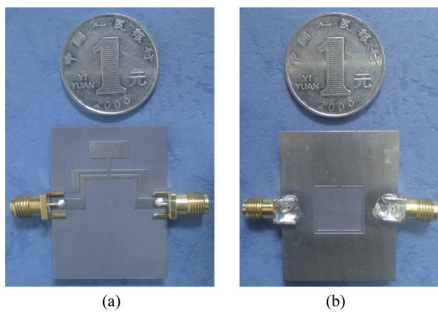


**Fig. 6.** Photographs of the fabricated dual-band BPF: (a) Top view. (b) Bottom view.

To verify the prediction, an experimental dual-band BPF based on the design approach is simulated and fabricated on the substrate with relative dielectric of 2.65 and thickness of 1 mm. The simulation was carried out using the EM simulation software ANSOFT HFSS, the input/output ports were ordinary 50Ω wave ports and the coaxial connectors were not included. Measurement was performed using a RS ZVM vector network analyzer. The

photographs of the proposed dual-band BPF are shown in Fig. 6. Its parameters are (unit: mm):  $W_0 = 2.8$ ,  $W_1 = 0.4$ ,  $W_2 = 0.4$ ,  $W_3 = 0.5$ ,  $W_6 = 1$ ,  $W_7 = 0.8$ ,  $W_8 = 2$ ,  $W_9 = 1$ ,  $W_{10} = 10$ ,  $L_1 = 13$ ,  $L_2 = 6$ ,  $L_3 = 5.9$ ,  $L_6 = 6.1$ ,  $L_9 = 6.8$ ,  $L_{10} = 5.8$ ,  $L_{11} = 3$ ,  $L_{12} = 4.4$ ,  $S_1 = 0.1$ ,  $S_2 = 0.1$ ,  $S_5 = 0.3$ ,  $S_6 = 0.5$ . The whole filter has a compact size of  $19.4 \times 22.6 \text{ mm}^2$  (about  $0.22\lambda \times 0.26\lambda$ , where  $\lambda$  is the guided wavelength of 50Ω transmission line at the center frequency of the first passband). The dual-band BPF operates at 2.4/3.2 GHz, with fractional bandwidths of 6.2/7.3% and measured minimal insertion losses of 2/0.9 dB (include the loss of the connectors). Three transmission zeros at 2.06, 2.6 and 3.44 GHz are generated to realize sharp roll-off performances, while an additional transmission zero at 4.11 GHz was introduced by the capacitive source load coupling to improve the upper stopband performance. A wide upper stopband with rejection better than 25 dB up to about 10 GHz was achieved. Some discrepancies are mainly attributed to the tolerance in fabrication and implementation.

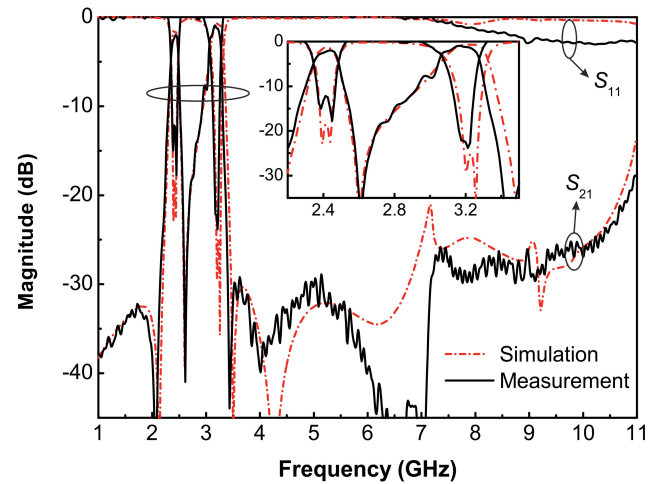


**Fig. 7.** Simulated and measured frequency responses of the fabricated dual-band BPF.

### 4. Conclusion

A novel type of compact and high selectivity dual-band BPF using the DDGSR and the DOLSIR is proposed. The DDGSR is suitable for designing the lower passband since it has a wideband spurious frequency suppression characteristic, which can generate a wide upper stopband and have little effect on the second passband generated by the other resonators. High selectivity of the first passband can be achieved by the inherent transmissions zero of the DDGSR and the additional one created by the capacitive source load coupling. The second passband can be designed using the DOLSIR with the same feed lines as the first passband. Moreover, the second passband frequency of the dual-band BPF can be easily shifted over a wide range, and it is convenient to allocate the inherent transmission zero in the higher side of the second passband to improve the upper stopband performance or in the lower side of the second passband to improve the isolation between the two passbands.

## References

- [1] TSAI, L. C., HSUE, C. W. Dual-band bandpass filters using equal-length coupled-serial-shunted lines and Z-transform technique. *IEEE Trans. Microw. Theory Tech.*, 2004, vol. 52, no. 4, p. 1111 - 1117.
- [2] MIYAKE, H., KITAZAWA, S., ISHIZAKI, T., YAMADA, T., NAGATOMI, Y. A miniaturized monolithic dual band filter using ceramic lamination technique for dual mode portable telephones. *IEEE MTT-S International Symposium Digest*. 1997, p. 789 - 792.
- [3] WU, B., LIANG, C.-H., QIN, P.-Y., LI, Q. Compact dual-band filter using defected stepped impedance resonator. *IEEE Microw. Wireless Compon. Lett.*, 2008, vol. 18, no. 10, p. 674-676.
- [4] WENG, M. H., HUANG, C. Y., WU, H. W., SHU, K., SU, Y. K. Compact dual-band bandpass filter with enhanced feed coupling structures. *Microw. Opt. Technol. Lett.*, 2007, vol. 49, no. 1, p. 171-173.
- [5] CHU, Q.-X., CHEN, F.-C. A compact dual-band bandpass filter using meandering stepped impedance resonators. *IEEE Microw. Wireless Compon. Lett.*, 2008, vol. 18, no. 5, p. 320-322.
- [6] CHANG, Y.-C., KAO, C.-H., WENG, M.-H., YANG, R.-Y. Design of the compact dual-band bandpass filter with high isolation for GPS/WLAN applications. *IEEE Microw. Wireless Compon. Lett.*, 2009, vol. 19, no. 12, p. 780-782.
- [7] ZHOU, M.-Q., TANG, X.-H., XIAO, F. Compact dual band bandpass filter using novel E-type resonators with controllable bandwidths. *IEEE Microw. Wireless Compon. Lett.*, 2008, vol. 18, no. 12, p. 779-781.
- [8] MONDAL, P., MANDAL, M. K. Design of dual-band bandpass filters using stub-loaded open-loop resonators. *IEEE Tans. Microw. Theory Tech.*, 2008, vol. 56, no. 1, p. 150-155.
- [9] ZHANG, X.-Y., SHI, J., CHEN, J.-X., XUE, Q. Dual-band bandpass filter design using a novel feed scheme. *IEEE Microw. Wireless Compon. Lett.*, 2009, vol. 19, no. 6, p. 350-352.
- [10] CHEN, C.-Y., HSU, C.-Y., CHUANG, H.-R. Design of miniature planar dual-band filter using dual-feeding structures and embedded resonators. *IEEE Microw. Wireless Compon. Lett.*, 2006, vol. 16, no. 12, p. 669-671.
- [11] LUO, X., QIAN, H.-Z., MA, J.-G., MA, K.-X., YEO, K. S. Compact dual-band bandpass filters using novel embedded spiral resonator (ESR). *IEEE Microw. Wireless Compon. Lett.*, 2010, vol. 20, no. 8, p. 435-437.
- [12] CHEN, J.-X., YUM, T. Y., LI, J.-L., XUE, Q. Dual-mode dual-band bandpass filter using stacked-loop structure. *IEEE Microw. Wireless Compon. Lett.*, 2006, vol. 16, no. 9, p. 502-504.
- [13] ZHANG, X.-Y., XUE, Q. Novel dual-mode dual-band filters using coplanar-waveguide-fed ring resonators. *IEEE Trans. Microw. Theory Tech.*, 2007, vol. 55, no. 10, p. 2183-2190.
- [14] BAIK, J.-W., ZHU, L., KIM, Y.-S. Dual-mode dual-band bandpass filter using balun structure for single substrate configuration. *IEEE Microw. Wireless Compon. Lett.*, 2010, vol. 20, no. 11, pp. 613-615.
- [15] HONG, J.-S., SHAMAN, H., CHUN, Y.-H. Dual-mode microstrip open-loop resonators and filters. *IEEE Trans. Microw. Theory Tech.*, 2007, vol. 55, no. 8, p. 1764-1770.
- [16] WANG, L., GUAN, B.-R. Compact dual-mode DGS resonators and filters. *Prog. Electromagn. Res. Lett.*, 2011, vol. 25, p. 47-55.
- [17] HONG, J.-S., SHAMAN, H., CHUN, Y.-H. Dual-mode microstrip open-loop resonators and filters. *IEEE Trans. Microw. Theory Tech.*, 2007, vol. 55, no. 8, p. 1764-1770.
- [18] ZHANG, X.-C., YU, Z.-Y., XU, J. Design of microstrip dual-mode filters based on source-load coupling. *IEEE Microw. Wireless Compon. Lett.*, 2008, vol. 18, no. 10, p. 677-679.

## About Authors ...

**Lei WANG** was born in the Jiangsu province of China. He received his BS degree from Xidian University in 2004 where he is pursuing his PhD degree. His research interests include defected ground structures and their application to microwave components and antennas.

**Bo-Ran GUAN** was born in Shandong province of China. He received his BS, MS, and PhD degree in the major of electromagnetic field and microwave technology from Xidian University in 1982, 1986 and 1990 respectively. He is now the head of the Institute of Antenna and Microwave in Hangzhou Dianzi University. His research interests include antenna propagation and microwave circuits.